Improving Synchronous Reluctance Machine Performance by Direct Capacitance Injection through an Auxiliary winding

A.S.O Ogunjuyigbe, A.A Jimoh, *member IEEE* and D.V Nicolae, *member IEEE*
Graduate School of Electrical and Electronic Engineering
Tshwane University of Technology, P.O.Box X680, Pretoria 0001
Email: Jimohaa@tut.ac.za, aogunjuyigbe@yahoo.com , danaurel@yebo.co.za

Abstract — Synchronous reluctance machine with a conventional rotor structure and a 3-phase auxiliary winding attached to a balanced capacitance for power factor improvement will find application in high speed , high power drives. This paper presents an understanding of its operation using the electromagnetic as well as the electric circuit concepts. Analytical and simulation results of this machine configuration show that the torque as well as the power factor performance is better compared to conventional reluctance machine.

Index Terms: Power factor improvement, Auxiliary winding, Synchronous Reluctance Machine, Capacitance Injection.

I. INTRODUCTION

The interest to use synchronous reluctance machine (Syncrel) for industrial application is at the moment increasing, because of the fact that this class of machine has the ability to withstand harsh environment, low inertia, high power to weight ratio, good acceleration performance and flux weakening operation [1-3]. These advantages motivated research on this machine for many decades, and it is now considered an economic alternative to its counterparts (Permanent Magnet, Induction Machine, Switched reluctance).

Various research efforts to improve the performance of this class of machine over the decades have been greatly focused on the rotor shape variations. This led to the emergence of the following rotor configurations: 1) Simple salient structure, 2) Segmented rotor type, 3) Flux barrier type, 4) Transversely laminated and 5) Axially laminated type.

Interestingly, these rotor configurations have gone through different design refinements to achieve a high saliency ratio (L_d/L_q) and high L_d-L_q. Some of the achievements on these rotor variations are reported in [2, 4-8]. Furthermore, as a build up on the rotor variations and designs, some research work [6, 9] exploited the advantages of multi-phase arrangements to develop a high torque performance machine using 5-phase arrangements rather than the traditional 3-phase. The torque performance of the 5-phase machine was further improved by controlling it to utilize the third harmonic components of current, and with a simple salient rotor structure a torque improvement of about 10% was reported. It is, however, not discussed how the power factor of the machine is improved with this arrangement.

The power factor (PF) can be improved typically by reactive power compensation through the installation of capacitor banks; however these capacitor banks have been found to result in problems particularly when there is a loss of supply. If these capacitors are series connected and external, it will ordinarily lower the overall impedance of the machine which will result in large currents and possibly a negligible improvement of power factor. On the other hand if it is shunt connected the power factor of the external supply is improved rather than the inherent power factor of the machine. Also the use of either of these methods can cause problem at light load conditions and relatively expensive switchgear is required to vary the capacitance value with the load changes [10]. Hence, these methods do not represent a useful practical method to improve the power factor of the machine. Techniques incorporating controlled switch in the stator winding have also been utilized, however this requires additional filtering since they were found to generate large harmonic currents in the machine as well as in the line [11, 12].

This paper then discusses a configuration to improve the performance of synchronous reluctance machine using a 3-phase auxiliary winding and capacitance injection. The Synchronous reluctance machine is equipped with two 3-phase stator windings identified as ‘abc’ and ‘xyz’. These two windings are electrically isolated but magnetically coupled. The first winding ‘abc’ is attached to the utility supply while the second winding ’xyz’ is directly connected to a balanced capacitance both for excitation and power factor improvement. The conceptual diagram of the machine is as shown in Fig. 1.

This machine will generally find application in the areas where salient pole synchronous reluctance machine is required. An example of this is the high power, high speed drives for petrochemical industry where arcing within the machine is not allowed [6].

The paper is organized as follows. Section II describes the principle of operation of this machine using the magnetic field concepts to describe the torque improvement as a result of the added winding and capacitance injection. The equivalent circuit suitable for dynamic, transient and steady state analysis of the machine was developed in the rotating dq reference frame in section III. Afterwards, a steady state analysis to show the power factor improvement, as well as the variation of the input current and electromagnetic torque of the machine for different load angles is presented in section IV. The paper is concluded in section V.

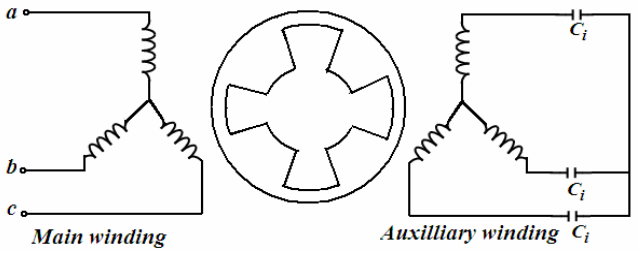

Fig. 1: Synchronous Reluctance machine with Auxiliary winding and Capacitance injection equivalent circuit analysis

II. PRINCIPLES OF OPERATION

The field approach is used in this paper to present a better understanding of the machine operation. The conceptual diagram of the machine is shown in Fig.1.

In the analysis that follows, it is assumed that the windings are sinusoidally distributed, and only the fundamental components of the winding distributions and currents are considered. Likewise, the rotor is assumed to have infinite permeability.

Given the characteristic of the machine structure under consideration in this paper, we have two magneto motive force (MMF) distributions.

If the main winding is excited by a balanced three phase current [14], then the resulting MMF by the balanced windings and balanced three phase current is:

$$F_{ga} = F_{ma}\cos(\omega_s t + \alpha - p\theta) \tag{1}$$

where ω_s is the angular frequency of the current in winding 'abc', and α is the phase angle of the main current and $F_{ma}=1.5N_mI_m$. Since the second winding 'xyz' are magnetically coupled to the winding 'abc', by transformer action an emf is induced in winding 'xyz'. Thus, a balanced three phase current (I_{xyz}) flows in the winding 'xyz'. However, this current is dependent on the size of capacitor attached to the winding 'xyz' and it is expressed as:

$$\left.\begin{aligned} I_x &= I_m \sin(\omega_s t + \alpha - \alpha_{aux}) \\ I_y &= I_m \sin(\omega_s t + \alpha - \alpha_{aux} - 2\pi/3) \\ I_z &= I_m \sin(\omega_s t + \alpha - \alpha_{aux} + 2\pi/3) \end{aligned}\right\} \tag{2}$$

These set of currents represented in equation (2) will similarly produce an MMF represented as:

$$F_{gx} = F_{mx}\cos(\omega_s t + \alpha - \alpha_{aux} - p\theta) \tag{3}$$

The rotor under consideration is a reluctance rotor without winding and does not carry current, then the total airgap magneto motive force (MMF) F_{gt} is given as:

$$F_{gt} = F_{ga} + F_{gx} = F_{ma}\cos(\omega_s t - \alpha - p\theta) + F_{mx}\cos(\omega_s t - \alpha - \alpha_{aux} - p\theta) \tag{4}$$

The reluctance rotor is usually designed to ensure a large variation of airgap permeance with respect to the angular position. It will develop torque because the magnetic stored energy changes if the rotor moves with respect to the stator MMF [13].

The stored energy in the magnetic circuit having a length *l* and radius *r* is given as:

$$E = rl\int_0^{2\pi} \mu_o g^{-1}(\theta,\phi_r)F_{gt}^2(\theta)d\theta \tag{5}$$

where $g^{-1}(\theta,\varnothing_r)$ represent the approximated inverse airgap length as defined in [1,13]; thus equation (5) resolves to:

$$E = \mu_o \pi rl[m(F_{ma}^2 + F_{mx}^2 + F_{ma}F_{mx}\cos\alpha_{aux}) + \frac{n}{2}(F_{ma}^2\cos(2\delta) + F_{mx}^2\cos(2\delta - \alpha_a) + F_{ma}F_{mx}\cos(2\delta + \alpha_a))] \tag{6}$$

The component parts of equation (6) which is dependent on the rotor angular position (δ) are the only one that participates in electromagnetic torque production. The torque is obtained from the rate of change of stored energy in the magnetic circuit with respect to the angular position, and is written as [13, 16]:

$$T_{av} = p_r\frac{dE}{d\delta} \tag{7}$$

Consequently, the torque expression for the machine configuration discussed in this paper is obtained using equation (7) and written as:

$$T_{av} = p_r\mu_o nr\pi l\left[\left(F_{ma}^2\sin(2\delta) + F_{mx}^2\sin(2\delta - 2\alpha_a) + F_{ma}F_{mx}\sin(2\delta + \alpha_a)\right)\right] \tag{8}$$

The first and second components of equation (8) indicate the torque contribution of the main and the auxiliary winding respectively, while the third component is the torque developed as a result of the interaction of the currents of the two windings.

The torque equation of a conventional Synchronous reluctance machine is given as [15]:

$$T_{rel} = p_r\mu_o nr\pi l F_{ma}^2\sin(2\delta) \tag{9}$$

A comparison of equations (8) and (9) shows the torque improvement to correspond to the sum of the second and third components of equation (8) thus:

$$T_{dif} = T_{av} - T_{rel} = p_r\mu_o nr\pi l\left[\left(F_{mx}^2\sin(2\delta - 2\alpha_a) + F_{ma}F_{mx}\sin(2\delta + \alpha_a)\right)\right] \tag{10}$$

This torque difference, equation (10), is easily observed to evolve as a result of the presence of the auxiliary winding with the capacitance connected to it. With proper design this can be optimized as a positive torque contribution. The variations of the torque T_{av} and T_{dif} (the improvement) as functions of the capacitance and load angle are discussed later on in section IV.

III. EQUIVALENT CIRCUIT ANALYSIS

A. *Machine Structure*

The conceptual diagram of the machine structure discussed in this paper is as shown in Fig. 1. The main winding 'abc' is connected to the mains supply while the auxiliary winding 'xyz' is connected to a capacitor that is utilized to inject a leading reactive power into the machine for power factor improvement. The two windings have the same number of poles and are sinusoidally distributed.

B. *Machine Mathematical Model*

The equations that describe the electrical behaviour of the machine structure are given as:

$$V_{abc} = R_s I_{abc} + \frac{d}{dt}\lambda_{abc} \tag{11}$$

$$V_{xyz} = R_s I_{xyz} + \frac{d}{dt}\lambda_{xyz} \quad (12)$$

where:

$$\lambda_{abc} = L_{abc} I_{abc} + L_{abcxyz} I_{xyz} \quad (13)$$

$$\lambda_{xyz} = L_{xyzc} I_{xyz} + L_{xyzabc} I_{abc} \quad (14)$$

gives the flux linkages of the windings.
L_{abc} and L_{xyz} represent the self and mutual inductances of each of the stator winding, while L_{abcxyz} and L_{xyzabc} represent the mutual inductances between the two windings. In matrix form, we can write

$$[\lambda_s] = [L_{ss}][I_s] \quad (15)$$

$$[\lambda_s] = \begin{bmatrix} \lambda_a & \lambda_b & \lambda_c & \lambda_x & \lambda_y & \lambda_z \end{bmatrix}^T \quad (16)$$

$$[I_s] = \begin{bmatrix} I_a & I_b & I_c & I_x & I_y & I_z \end{bmatrix}^T \quad (17)$$

$$L_{ss} = \begin{bmatrix} L_{abc} & L_{abcxyz} \\ L_{xyzabc} & L_{xyz} \end{bmatrix} \quad (18)$$

where :

$$L_{abc} = \begin{bmatrix} L_{aa} & L_{ab} & L_{ac} \\ L_{ba} & L_{bb} & L_{bc} \\ L_{ca} & L_{cb} & L_{cc} \end{bmatrix}; L_{xyz} = \begin{bmatrix} L_{xx} & L_{xy} & L_{xz} \\ L_{yx} & L_{yy} & L_{yz} \\ L_{zx} & L_{zy} & L_{zz} \end{bmatrix} \quad (19)$$

$$L_{abcxyz} = L_{xyzabc}^T = \begin{bmatrix} L_{ax} & L_{ay} & L_{az} \\ L_{bx} & L_{by} & L_{bz} \\ L_{cx} & L_{cy} & L_{cz} \end{bmatrix} \quad (20)$$

The self and mutual inductances in (18)-(20) are evaluated using the method of winding function theory and is given as

$$L_{ij} = (\mu_o \times r \times l) \int g^{-1}(\phi, \theta_{rm}) N_i(\phi, \theta_{rm}) N_j(\phi, \theta_{rm}) d\phi \quad (21)$$

where $N_i(\phi, \theta_{rm})$, $N_j(\phi, \theta_{rm})$ is the winding distribution functions for windings *i* and *j*.

The inductance components of (18)-(20) obtained using (21) are time varying, thus the voltage equations of (11) and (12) are time varying and this will actually be complicated to resolve. Thus using the transformation, and multiplying equations (11) and (12) by the appropriate transformation matrix *T(θ),* we can write

$$T(\theta) V_{abc} = R_s T(\theta) I_{abc} + T(\theta) \frac{d\lambda_{abc}}{dt} \quad (22)$$

$$T(\theta) V_{xyz} = R_s T(\theta) I_{xyz} + T(\theta) \frac{d\lambda_{xyz}}{dt} \quad (23)$$

and

$$T(\theta)\lambda_{xyz} = T(\theta) L_{abc} T(\theta)^{-1} T(\theta) I_{abc} + T(\theta) L_{abcxyz} T(\theta)^{-1} T(\theta) I_{xyz} \quad (24)$$

$$T(\theta)\lambda_{xyz} = T(\theta) L_{xyz} T(\theta)^{-1} T(\theta) I_{xyz} + T(\theta) L_{xyzabc} T(\theta)^{-1} T(\theta) I_{abc} \quad (25)$$

For which equations (22)-(25) can be written as:

$$V_{qd01} = R_s I_{qdo1} + \frac{d\lambda_{qd01}}{dt} - \omega\lambda_{qd01} \quad (26)$$

$$V_{qd02} = R_s I_{qdo2} + \frac{d\lambda_{qd01}}{dt} - \omega\lambda_{qd02} \quad (27)$$

and

$$\lambda_{qd01} = L_{qd01} I_{qd01} + L_{qd012} I_{qd02} \quad (28)$$

$$\lambda_{qd02} = L_{qd021} I_{qd01} + L_{qd02} I_{qd02} \quad (29)$$

Based on equations (26)-(29), the dq equivalent circuit of Fig. 2 is suggested.

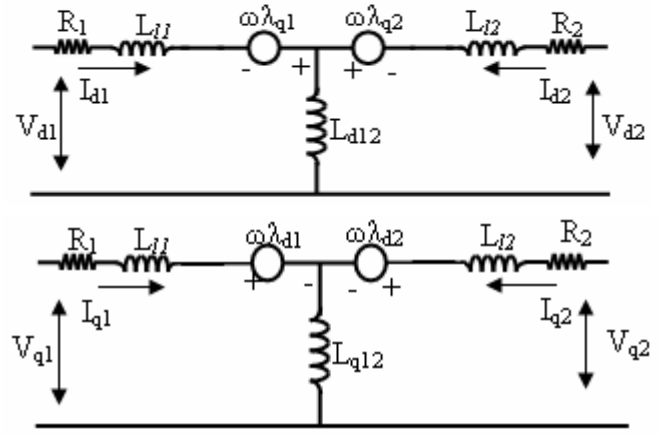

Fig. 2: DQ equivalent circuit of the machine

C. *Per Phase Equivalent circuit*

The complex form of equations (26)-(29) can be expressed as:

$$V_{qd01} = R_s I_{qdo1} + \frac{d\lambda_{qd01}}{dt} - j\omega\lambda_{qd01} \quad (30)$$

$$V_{qd02} = R_s I_{qdo2} + \frac{d\lambda_{qd01}}{dt} - j\omega\lambda_{qd02} \quad (31)$$

and

$$\lambda_{qd01} = L_1 I_{qd01} + L_m I_{qd02} \quad (32)$$

$$\lambda_{qd02} = L_m I_{qd01} + L_2 I_{qd02} \quad (33)$$

Under the steady state condition, the state derivatives of equations (30), (31) are set equal to zero; thus substituting (32), (33) into (30), (31), the resulting steady state equation is given by:

$$V_{qd01} = R_1 I_{qdo1} + j\omega(L_1 - L_m) I_{qdo1} + j\omega L_m (I_{qdo1} + I_{qdo2}) \quad (34)$$

$$V_{qd02} = R_2 I_{qdo2} + j\omega(L_2 - L_m) I_{qdo2} + j\omega L_m (I_{qdo1} + I_{qdo2}) \quad (35)$$

Applying appropriate transformations to equations (34) and (35), per phase equivalent equations of the machine can be written as:

$$V_a = R_1 I_a + j\omega L_{l1} I_a + j\omega L_m (I_a + I_x) \quad (36)$$

$$V_x = R_2 I_x + j\omega L_{l1} I_x + j\omega L_m (I_a + I_x) \quad (37)$$

From which we can draw the steady state per phase equivalent circuit of the machine as:

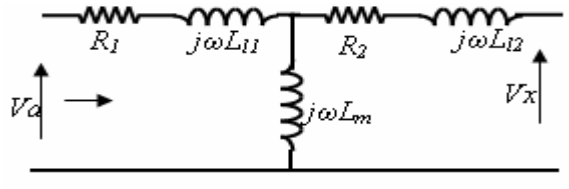

Fig. 3: Per phase steady state equivalent circuit

In view of the fact that the auxiliary winding 'xyz' is attached to a balanced capacitor as indicated in the conceptual diagram of Fig. 1, the per phase equivalent circuit is then drawn to include the capacitance C_i attached to winding 'xyz' as shown in Fig. 4.

This per phase representation suffices to study the use of solid state excitation/ PWM inverter for the capacitance injection particularly when the PWM is controlled to pass only reactive power [6].

IV. STEADY STATE ANALYSIS

The resulting per phase equivalent circuit of Fig. 4 is used here to examine the performance characteristics of the machine.

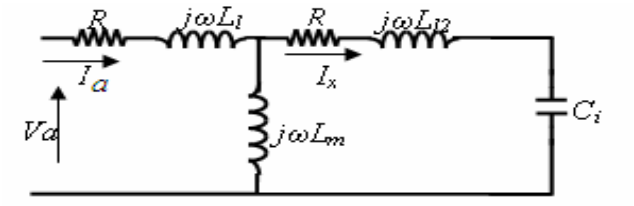

Fig. 4: Per phase equivalent circuit with the capacitance

The machine when viewed from the main winding presents the total input impedance Z_T that is expressed as:

$$Z_T = \left((R + jX_{l1}) + \left(X_m // (R + j(X_{l2} - X_c)\right)\right) \tag{38}$$

where $X_{l1} = X_{l2} = X_1 - X_m = X_1(1-k)$ and k is the coefficient of coupling. Hence, the total impedance can be written as:

$$\left.\begin{aligned} Z_T &= (R + jX(1-k)) + \frac{jkX \times (R + jX(1-k) - jX_c)}{jkX + R + jX(1-k) - jX_c} \\ &= R_{eq} + jX_{eq} \end{aligned}\right\} \tag{39}$$

The synchronous impedance of the kind of machine discussed in this work is expressed as [1]:

$$X = \tfrac{1}{2}(X_d + X_q) + \tfrac{1}{2}(X_d - X_q)e^{j2\delta} \tag{40}$$

This is written for simplicity of analysis as:

$$X = X_a + jX_b \tag{41}$$

At a specific load angle δ, the circuit of Fig. 4 will operate at unity power factor only when the imaginary part of the total input impedance (Z_T) becomes zero. Using (41) in (39), the imaginary part of the input impedance (Z_T) is obtained as:

$$\mathrm{Img}\, Z_T = \frac{(2RX_a - RX_c + X_bX_c - 2X_aX_b(1-k^2))(R - X_b) - (R^2 - 2RX_b + X_aX_c - (X_a^2 + X_b^2)(1-k^2))}{(R - X_b)^2 + (X_a - X_c)^2} \tag{42}$$

In order to achieve unity power factor, equation (42) is set to zero to obtain:

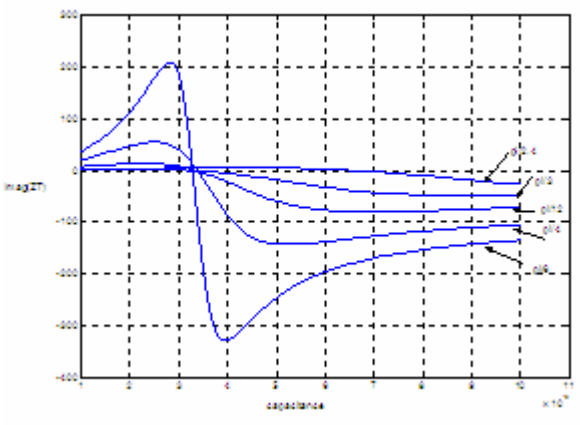

Fig. 5: Plot of the imaginary part of total impedance versus capacitance at different δ.

$$\begin{aligned} &X_aX_c^2 + ((1-k^2)(X_b^2 - X_a^2) - X_a^2 - X_b^2)X_c + R^2X_a + \\ &(1-k^2)(X_a^3 - X_aX_b - 2RX_aX_b + 2X_aX_b^2) = 0 \end{aligned} \tag{43}$$

Equation (43) can be compared to a quadratic equation of the form:

$$aX_c^2 + bX_c + c = 0 \tag{44}$$

where

$$\left.\begin{aligned} a &= X_a \\ b &= ((1-k^2)(X_b^2 - X_a^2) - X_a^2 - X_b^2) \\ c &= R^2X_a + (1-k^2)(X_a^3 - X_aX_b - 2RX_aX_b + 2X_aX_b^2 \end{aligned}\right\} \tag{45}$$

and a, b, c are constants at a given load angle.

This equation will have a solution for X_c only if $b^2 - 4ac \geq 0$.

From equations (39) and (43), the possibility of unity power factor is examined. The variation of the imaginary part of Z_T with the capacitance for different load angles is evaluated and plotted in Fig. 5. The possibility of unity power factor is observed for the different load angles considered. This additionally indicates that for a typical Synchronous reluctance using the arrangement discussed in this paper, unity power factor is possible over a wide range of load angle.

A. Impact of the Scheme on Power Factor

For a conventional synchronous reluctance machine with the same machine size and saliency ratio as that of the modified machine discussed in this paper, the power factor is evaluated to be 0.76. However, with the auxiliary winding attached to a balanced capacitance, the power factor (PF) of the modified machine can easily be controlled for different load situations, and it is evaluated using:

$$\cos\varphi = \frac{R_{eq}}{\sqrt{R_{eq}^2 + X_{eq}^2}} \tag{46}$$

Figs. 6, 7, and 8 shows the plots of the power factor of the modified machine as function of capacitance and load angle, while Fig. 9 and 10 show respectively the plots of the main winding current versus the power factor angle and a contour plot of the main winding currents as a function of capacitance and load angle.

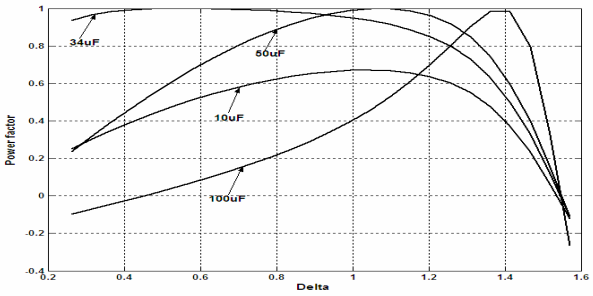

Fig. 6: Plot of PF versus δ at varying capacitance values

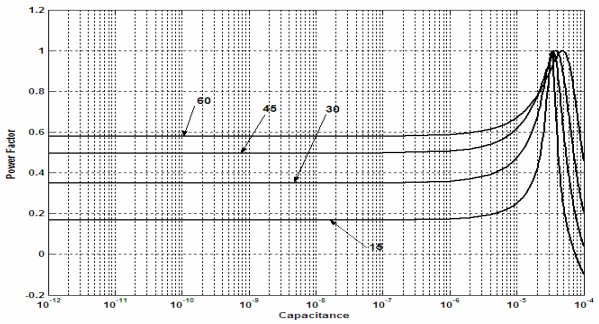

Fig. 7: Logarithmic plot of PF versus capacitance at varying δ.

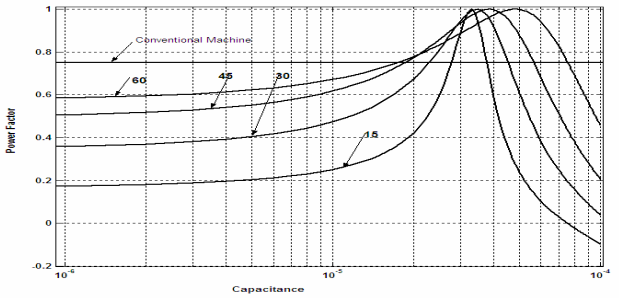

Fig. 8: Improvement in PF compared with the conventional machine

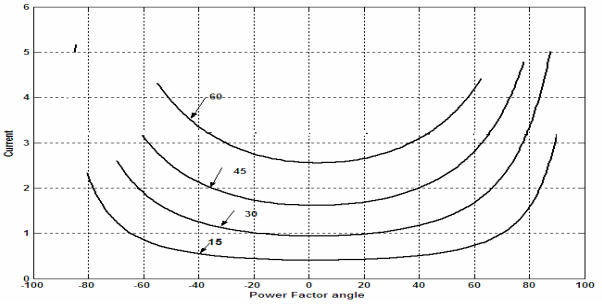

Fig. 9: Plot of the main winding current against the PF angle.

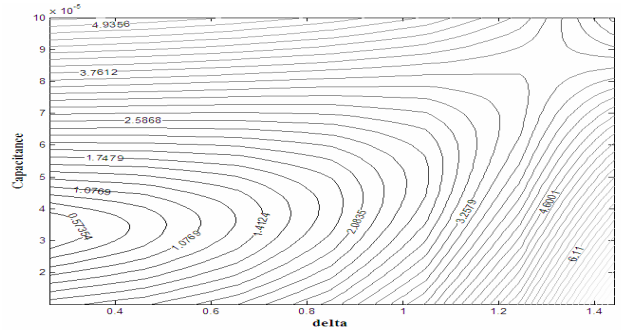

Fig. 10: Contour plot of the variation of the main winding current as a function of capacitance and δ

These figures clearly illustrate the possibility of operating this machine at unity power factor for different load angles as well as capacitance values. The figures also further illustrate that unlike the conventional synchronous reluctance machine, the modified machine has a relatively high power factor over a wide range of load angles. This is due to the presence of the auxiliary winding and the capacitance injected which influences the current to either leading or lagging. It is also evident from Fig. 9 and 10 that the points where high power factor are possible for different load angles correspond to the points of minimum current in the main winding.

B. Impact of the Scheme on Torque

At steady state, the electromagnetic torque (T_{em}) developed by the modified machine is evaluated using [3, 14]:

$$T_{em} = \frac{3V^2 R_{eq}}{R_{eq}^2 + X_{eq}^2} \tag{49}$$

The variation of the torque as a function of the capacitance injected and the load angle is displayed respectively in the logarithmic plots of Figs. 11 and 12. The torque-load angle curve for the machine with and without the modification is displayed in Fig.12, while Fig. 13 and 14 gives the change in torque as a result of the modification carried out on the machine.

As evident in Fig. 11, the variation of the torque developed with the capacitance injected in the modified machine follows a similar pattern for the different load angles considered. The torque shows an initial increase particularly between 1μF and 40μF. However, it suddenly begins to decrease with a further increase in the capacitance.

The changes in the torque developed by this machine as a result of the modification were evaluated at different capacitance and load angles. These are illustrated in Fig. 13 and 14.

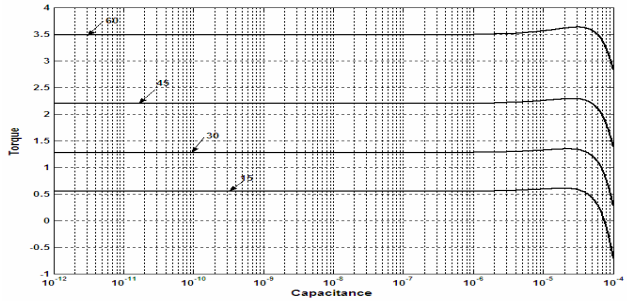

Fig. 11: Logarithmic plot of torque versus capacitance at varying δ

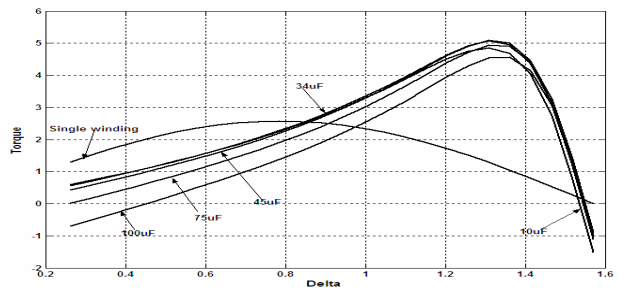

Fig. 12: Comparative plot of torque against δ varying capacitance

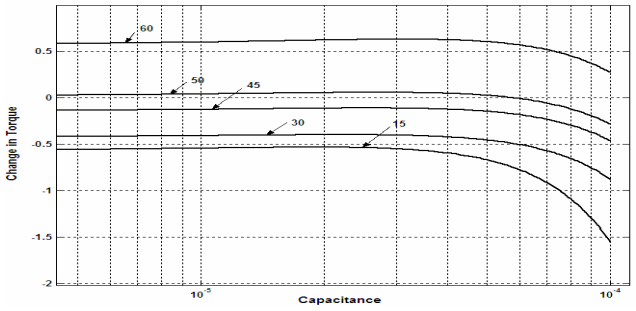

Fig. 13: Change in torque against capacitance at varying δ

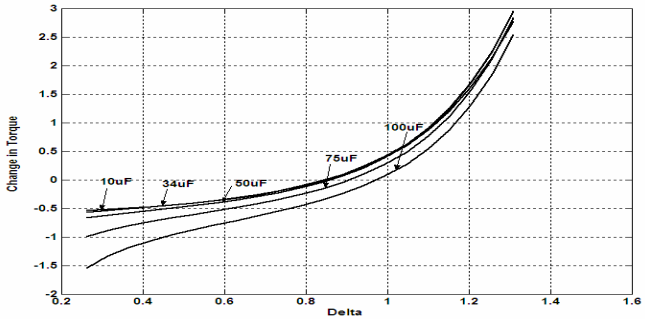

Fig. 14: Change in torque against δ at varying capacitance

It became essentially obvious from the curves of Figs.12 - 14 that the relative improvement in torque of the modified machine is at a load angle of 48º and higher. This improvement is also observed to be more obvious at an increased load angle. Furthermore, it can be seen from Fig. 8 and 14 that a high power factor (with the possibility of unity) are obtained at the load angles that corresponds to the ones where torque improvement is identified.

V. CONCLUSION

The use of direct capacitance injection through an auxiliary winding for the performance improvement of synchronous reluctance machine has been demonstrated. The principle have been explained using the field approach and the per phase steady state equivalent circuit showing machine parameters.

The torque equation as obtained from the field approach clearly suggest that for machine of the same dimensions, the output torque of this machine at typical load angle is higher than that of the conventional machine. The relative torque of the modified machine is found to be particularly improved only at load angle of 48º and higher.

Steady state plots that illustrate how the torque, power factor, reactive power and input current of this machine varied with the capacitor at different load angles were presented. In addition the condition, as well as the possibility of unity power factor over a wide range of load angles was shown.

With the known advantages and application area of synchronous reluctance machine, the scheme discussed in this paper should find acceptability particularly with better rotor design options.

VI. REFERENCES

[1] L.A. Agu, L.U. Anih, J, O. Ojo, and A.A. Jimoh,. '*Novel Synchronous reluctance machines with Capacitance Injection'*. LH Marthinusen Rotating Machine Conference, Pilansberg Conference centre, South Africa. pp.1-8

[2] F. Parasitili, M. Villani and A. Tassi, '*Dynamic Analysis of Synchronous Reluctance Motor Drives Based on Simulink and Finite Element Model'* IEEE Industrial Electronics, IECON Nov. 2006.

[3] E.S Obe, and T. Senjyu, '*Analysis of a polyphase synchronous reluctance motor with two identical stator windings'* EPSR 76. pp 515-524. 2005.

[4] A. Chiba, T. Fukao and M. Matsui, *Test Results on a Super High Speed Amorphous Iron Reluctance Motor*. IEEE Transactions on Industry application, Vol. 25, No.1 pp.119-125. 1989

[5] T. Matsuo, and T.A. Lipo, '*Rotor Design Optimization of Synchronous Reluctance Machine'*. IEEE Transaction on Energy Conversion, Vol. 9, No.2, pp 359-365. 1994.

[6] E.T. Rakgati and M.J Kamper, '*Torque Performance of Optimally designed three- and Five Phase Reluctance Synchronous Machine'*. SAIEE Vol. 97(1), pp 43-49.2006.

[7] T. A.. Lipo, *Novel Synchronous Reluctance Concepts for Variable Speed Drives*. IEEE-IAS Annual meeting. pp 34-43.1991.

[8] V.B Honsinger, *'Steady state performance of reluctance machines ',* IEEE Trans. On Power Apparatus and Systems, Vol.PAS-90, pp.305-311, Jan./Feb. 1971.

[9] H.A. Toliyat, P.W. Shaleish, and T. Lipo, , 'Analysis *and simulation of five phase Synchronous reluctance machines including Third Harmonic of Airgap MMF'* IEEE Transactions on Industry Applications, Vol.34, No. 2. pp 332-3390 (1998)

[10] E. Mujaldi, T.A. Lipo, and D.W. Novotny, '*Power Factor enhancement of Induction Machines by means of solid state excitation'*, Research report 86-3 of WEMPEC. 1986.

[11] M. Suchi, P .Kansara, and W. Szabo, 'Performance Enhancement of an Induction Motor by Secondary Impedance Control', IEEE Trans. On Energy Conversion, Vol. 17, No. 2 June 2002.

[12] D.V. Nicolae and A.A Jimoh, '*A Three Phase Induction Motor with power electronic controlled Single Phase Auxiliary Stator winding*' PECS 2007.

[13] E. Spooner and A.C Williams, '*Mixed Pole Windings and some Applications',* IEE Proceedings, Vol. 137, Pt. B, no. 2 March 1990. pp 89-97.

[14] P.C. Krause '*Analysis of Electric Machinery'* McGraw-Hill Book Company.

[15] C.B. Gray, *Electrical Machines and Drives,* Longman Scientific and Technical England. 1989

[16] O. Ojo, Gan Dong, and M.O. Omoigui, '*Analysis of a Synchronous Reluctance Machine with an Auxiliary Single-Phase Winding'* IEEE Transactions on Industry Applications, Vol. 39, No. 5 Sept/Oct.2003.pp 1307-1313.